RSC Advances

ROYAL SOCIETY OF CHEMISTRY

www.rsc.org/advances

Graphic abstract for:

A small-molecule chemosensor for the selective detection of 2,4,6-trinitrophenol (TNP)

Jianting Pan[a], Fang Tang[a], Aixiang Ding[a], Lin Kong[a]*, Longmei Yang[a], Xutang Tao[b], Yupeng Tian[a], Jiaxiang Yang[a,b,]*

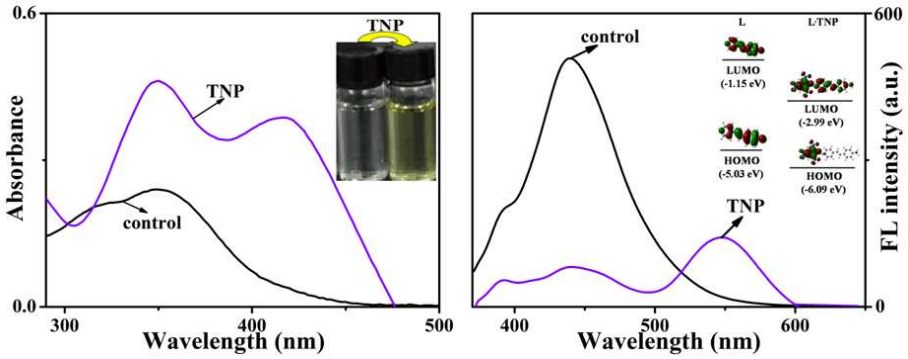

A pyridine-based small-molecule receptor (**L**) for specific recognition of TNP was synthesized and characterized by ^{1}H NMR, ^{13}C NMR and FT-IR spectra, the optical properties were studied by UV-Vis absorption and PL spectra. The results showed that the fluorescence of **L** was strongly quenched by picric acid, accompanying with an obviously color change from transparent to yellow, which indicated that receptor **L** can serve as a small-molecule sensor for TNP. The crystal structure and theoretical calculation of corresponding host-guest complex **L**·**TNP** were also performed.

RSC AdvancesRSCPublishing

PAPER

cweizhiCite this: DOI: 10.1039/x0xx00000x

A small-molecule chemosensor for the selective detection of 2,4,6-trinitrophenol (TNP)

Jianting Pan[a], Fang Tang[a], Aixiang Ding[a], Lin Kong[a]*, Longmei Yang[a], Xutang Tao[b], Yupeng Tian[a], Jiaxiang Yang[a,b,]*

Received 00thxxxxxxxx,
Accepted 00thxxxxxxxx

DOI: 10.1039/x0xx00000x

www.rsc.org/

A pyridine-based small-molecule receptor (**L**) for specific recognition of TNP was synthesized and characterized by ^{1}H NMR, ^{13}C NMR and FT-IR spectra, the optical properties were studied by UV-Vis absorption and PL spectra. The results showed that the fluorescence of **L** was strongly quenched by picric acid, accompanying with an obviously color change from transparent to yellow, which indicated that receptor **L** can serve as a small-molecule sensor for TNP. The crystal structure and theoretical calculation of corresponding host-guest complex **L**·**TNP** were also performed.

Rational design and synthesis of host molecules for the particular guest molecules or ions are drawing more and more active attention due to their vitally important applications in the fields of biological and environmental sensing.[1,2] The structure of molecule possesses pyridine unit could be fascinating "acceptor" for a variety of metal ions for their strong binding abilities.[3,4] However, to our best knowledge, there still are rare reports focused on the neutral molecules of nitrated explosives, using trinitrophenol (TNP) as an example.[5,6] Nitro-aromatic compounds (NACs), such as 2, 4-dinitrotoluene (DNT), trinitrotoluene (TNT), TNP, to name a few, are widely used in manufacturing and blasting industries. Because of the potential damage to respiratory system and superior fierce explosive to that of TNT.[7,8,9] Apart from its highly explosive nature, TNP is also recognized as a infamous threat to the human health and national security, which can cause severe irritation, skin allergy, dizziness, nausea, damage of liver, and kidney.[10,11] Water contamination of TNP may cause severe epidemic.[12,13] As such, a large number of molecular and modulated chemosensors had been developed.[14-19] Some of them showed good selectivity and sensitivity to TNP, but their structures are complicated and usually need a multi-step and inefficient synthetic procedure. Therefore, developing simple and effective molecules for the specific recognition of TNP is urgent and instructive.

Herein, in our present paper, a novel simple pyridine-based compound, (E)-4-(2-(pyridin-4-yl)vinyl)aniline (**L**), was designed, synthesized and characterized, which was expected to form "host-guest" complex with TNP, giving entirely different UV-Vis absorption and fluorescence responsive. The absorption of compound **L** with TNP at 350 nm obviously increased, together with the appearance of a new strong absorption band at 424 nm, meanwhile, an apparent color change from transparent to yellow was observed, accompanying with a fluorescence quenching at 440 nm and a new emission band appearing at 550 nm.

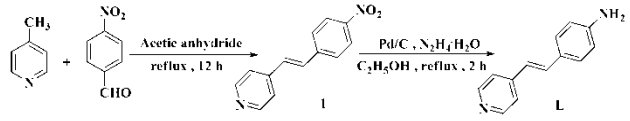

Scheme 1. Synthesis routes of receptor **L**.

Experimental section

Chemical and instruments

The commercially available chemicals were used without further purification. All of the solvents used were purified by conventional methods before use. Synthetic routes were shown in scheme 1 and the characterizations were described. ^{1}H NMR and ^{13}C NMR spectra were recorded on Bruker Avance 400 MHz NMR spectrometer, using DMSO-d_6 as solvent and calibrated using tetramethylsilane (TMS) as an internal reference. Data were reported as follows: chemical shifts (δ) in ppm, multiplicity (s = singlet, d = doublet, t = triplet, m = multiplet), coupling constants J (Hz), integration, and interpretation. The UV-Vis absorption spectra were recorded on the UV-265 spectrophotometer with a quartz cuvette (path length, 1 cm). The one-photon excited fluorescence (OPEF) spectra measurements were performed using the Hitachi F-7000 fluorescence spectrophotometer. High-resolution mass spectra (HR-MS) were taken on a Thermo Fisher

LTQ-Orbitrap XL mass Spectrometer using an electrospray ion source (ESI). FT-IR spectra were obtained in KBr discs on a Nicolet 380 FT-IR spectrometer in the 4000-400 cm^{-1} region. Photo images were obtained using a digital camera (Nikon D7000). Silica gel 60 (60-120 mesh) was used for column chromatography.

Caution! TNP, TNT, DNT, and other nitroaromatics (**a**~**h**, Fig. 1(c)) should be used with extreme care using the best safety precautions owing to their highly explosive character. They should be handled only in small quantities.

Preparation of the target compound L

Compound **L** was prepared according to the method reported in the literature.[20] FT-IR (KBr, cm^{-1}) selected bands: 3390 (m), 3317 (m), 3032 (w), 2923 (w), 2849 (w), 1584 (s), 1515 (s), 1415 (s), 832 (s). ^{1}H NMR (DMSO-d_6, 400 MHz, ppm) δ: 5.45 (s, 2H), 6.55 (d, J = 5.6 Hz, 2H), 6.83 (d, J = 5.4 Hz, 1H), 7.31 (m, 3H), 7.41 (d, J = 4.0 Hz, 2H), 8.42 (d, J = 4.0 Hz, 2H). ^{13}C NMR (DMSO-d_6, 100 MHz, ppm) δ:116.87, 122.91, 123.27, 126.17, 131.59, 132.87, 136.85, 148.35, 152.88. HR-MS (ESI-MS): m/z = 197.1107, calcd for $[C_{13}H_{13}N_2]^+$ = 197.1000 ($[M+H]^+$).

Results and discussion

UV-Vis absorption and fluorescence spectra

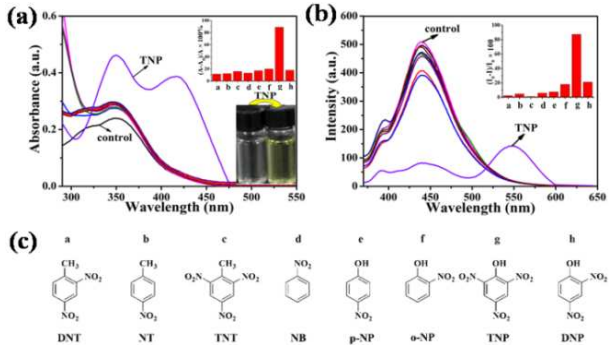

Fig. 1. (a) UV-Vis absorption of **L** (10 μM) in THF upon addition of 5 equiv. selected NACs. Inset: the degree of change in absorbance of 350 nm. A_0 is the absorbance of the receptor **L**, A is the absorbance after adding **a**-**h**. The photo shows that **L** appeared an obvious selectivity of TNP. (b) Responses of the **L** (10 μM) toward different NACs (5 equiv.) in THF. Inset: the degree of change in intensity of 440 nm. I_0 is the intensity of the receptor **L**, I is the intensity of **L** after adding **a**~**h**. (c) Structures of the NACs used in the present study (**a**~**h**).

Initially, the molecular recognition behaviors of the compound **L** toward the selected NACs were investigated by UV-Vis and fluorescence spectroscopy. As shown in Fig. 1(a), the free **L** in THF showed a maximum absorption wavelength at 350 nm. The influences of the selected NACs on its absorption were studied with the method as used before.[21] The addition of 5 equiv. TNP into compound **L** effected the absorption comparing with other NACs. The absorption of compound **L** with TNP at 350 nm evidently increased, accompanying the appearance of a new strong absorption band at 424 nm, which indicated there may be a formation of the complex between compound **L** and TNP with totally different electronic properties from that of compound **L**. Thanks to this, an obviously color change from transparent to yellow was observed after addition of TNP into compound **L**, allowing colorimetric detection of TNP by the naked eye (Fig. 1, insets).

Furthermore, fluorescence studies of the compound **L** with different NACs were shown in Fig. 1(b). The free **L** displayed an intensive emission at 440 nm in THF solution. The fluorescent influences of the NACs aginst **L** were also investigated in THF solution. It could be found that emission intensity of the compound **L** at 440 nm decreased dramatically (about 87% quenching) with a new emission wavelength at 550 nm when 5 equiv. TNP was added, however, negligible changes in the fluorescent spectra were monitored upon addition of other NACs. The above mentioned UV-Vis absorption studies and the fluorescent studies here demonstrated that compound **L** could bind with TNP effectively and serve as specific recognizer of TNP.

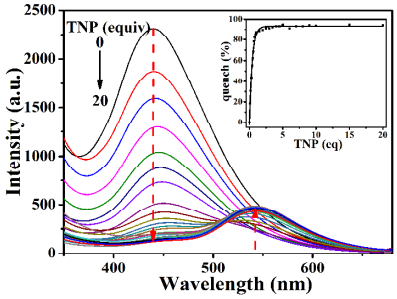

Fig. 2. Change in the fluorescence of the compound **L** (10 μM) in THF upon the addition of TNP (0-20 equiv.), λ_{ex} = 350 nm. Inset: the fluorescent quenching percentage as a function of TNP concentration, concentration = 10 μM.

In order to get a further investigation to the photo-physical response of the compound **L** with TNP, corresponding UV-Vis titration experiment (Figure S1, ESI†) and fluorescent titration experiment were conducted. As shown in Fig. 2, upon addition of incremental amounts of 10 μM of TNP to the solution of **L** in THF, the quenching in fluorescence emission at 440 nm was observed at concentration as low as 20 equivalents. Meanwhile, a new emission at 550 nm rose up. Then we measured fluorescence lifetime of derivative **L** for different concentrations of TNP (0, 0.5, 1.0 equiv.). The fluorescence lifetime of compound **L** was found to be invariant (< 0.1 ns) at different concentration of TNP (Figure S2, ESI†). Thus, indicating that the quenching at 440 nm is static and ground state complex is formed between compound **L** and TNP. These results implied that there are strong interaction between **L** and TNP. We proposed that three "NO_2" groups in TNP may act as strong electron-withdrawing group protonating the pyridine ring to further affect the intramolecular electron density distribution when they formed hydrogen bond interaction

by each other. The redistribution of the electron density influenced the intramolecular charge transfer (ICT) that subsequently induced an absorption and fluorescence response to TNP. Job's plot analysis was conducted to corroborate 1:1 ratio between **L** and TNP (Figure S3, ESI†).[22] A linear Stern-Volmer plot was obtained from fluorescence quenching titration (Figure S4, ESI†) with $K_{SV} = 4.106 \times 10^5\ M^{-1}$.[9] The detection limit was also found to be 400 ppb for TNP (Figure S5, ESI†).[23] The interference experiment of other nitro aromatics towards the interaction of TNP with **L** in THF was conducted (Figure S6, ESI†), it was found that the fluorescence emission intensity of the **L** was almost unaffected. Considering an environmental application, an optimized aqueous solution (THF : H_2O = 9 : 1, v/v) was then selected as a testing system to investigate the spectral response of the probe **L** to TNP at room temperature. As shown in Figure S7 (ESI†), both the absorption and fluorescence spectra in aqueous solution gave a similar response to those observed in pure THF, proving that **L** can detect TNP in aqueous solution. The ideal experimental results here amplified the practical applicability of the probe toward TNP sensing. Further, we did the fluorescence titration experiments of the probe **L** to TNP (0-20 equiv.) at various excitation wavelengths. No obvious change in quenching efficiency of TNP was observed (Figure S8, ESI†).

Single crystal analysis

Next, we grew the single crystal of **L·TNP** and investigated the interactions between the **L** and TNP to explain the emission band changing. When 5 mL of TNP (2.6×10^{-2} M) solution was added to 5 mL of **L** (2×10^{-2} M) solution in THF/ethanol (2:1). After a few days, vermilion block crystals were obtained by slow evaporation of the solvent at room temperature (Fig. 3a). A single-crystal X-ray diffraction analysis revealed that a 1:1 host-guest complex **L·TNP** was formed (Fig. 3a) by **L** and TNP as in solution. The relevant crystal data and structural parameters were listed. (Table 1) All calculations and graphical works have been done using WinGX[24] and PLATON[25] programs.

Table 1 Summary of crystallographic data and structure refinement details for L·TNP

Identification code	**L·TNP**
Empirical formula	$C_{19}H_{15}N_5O_7$
Formula mass	425.36
Crystal system, Space group	Monoclinic, *P2(1)/c*
Unit cell dimensions	$a = 7.917(5)$ Å
	$\alpha = 90.000(5)$ °
	$b = 12.258(5)$ Å
	$\beta = 96.658(5)$ °
	$c = 20.049(5)$ Å
	$\gamma = 90.000(5)$ °
Volume	1932.6(15) Å^3
Z, *Calculated density*	4, 1.462 Mg·m^{-3}
Temperature	298(2) K
Crystal size	0.30 × 0.20 × 0.20 mm
Absorption coefficient	0.115 mm^{-1}
F(000)	880
Theta range for data collection	1.95 ° to 25.00 °
Limiting indices	$-9 \le h \le 7$
	$-14 \le k \le 14$
	$-23 \le l \le 23$
Reflections collected	9806/3417
Data / restraints / parameters	3417/1/280
Goodness-of-fit on F^2	1.032
Final R indices [I>2sigma(I)]	*R1* = 0.0802, *wR2* = 0.1862
R indices (all data)	*R1* = 0.1211, *wR2* = 0.2164

The crystal structure showed that the nitrogen of the pyridine group of **L** is protonated to form as a cation while picric acid is deprotonated to form as a anion, where the pyridine group was changed from a hydrogen bond acceptor to the hydrogen bond donor (Fig. 3a).[26] The "**L** cations" and "TNP anions" were self-assembled to form a supramolecular structure *via* multiple hydrogen bond and π-π interactions. As shown in Fig. 3b and c, each picrate acted as a hydrogen bond acceptor to connect six ligands and one picrate *via* 8 hydrogen-bonds, and each **L** acted as hydrogen bond donor and acceptor to connect seven picrates and one other ligand *via* 8 hydrogen bonds in which the D-A distances vary from 2.763 to 3.591 Å and the corresponding D-H···A angles were in the range 118.53-171.29 ° (Table S1, ESI†). The intermolecular π-π stacking interaction between the picrate ring and phenylamine ring of **L**, presented a π-π distance of 3.859 Å and a dihedral angle of 15.8 °. It was noteworthy that the two hydrogen bonds between N4 of the pyridine group bonding to the O7 of the hydroxyl group and the O5 of the nitro group in the picrate respectively were very strong owing to their short distance.[27] These results implied that the pyridine group of **L** was the key site for specific interaction with TNP.

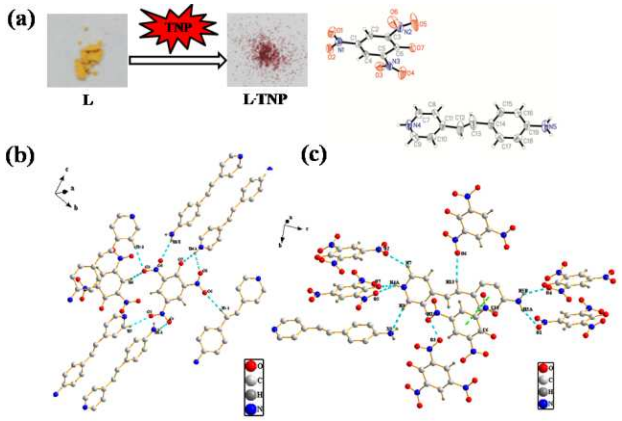

Fig. 3. (a) Photos of **L** and **L·TNP** and the X-ray structure of the host-guest complex **L·TNP**; (b) The hydrogen bond interactions around TNP in the complex; (c) The hydrogen bond interactions and π-π interactions around **L** in the complex (the hydrogen bond interactions and π-π interactions are indicated with dashed turquoise and bright green lines, respectively. Some hydrogen atoms are omitted for clarity).

^{1}H NMR titration

The interaction between the probe **L** and TNP in solution was further studied by the method of ^{1}H NMR titration experiment (Fig. 4). The signals of the hydrogens located on the aromatic

rings were generally downfield shifted upon addition of 2.0 equiv. TNP. Due to the decrease in electron density of the pyridine ring moiety, Hb, Hc and Hf were shifted obviously, and the chemical shifts (Δδ) for **L** were 0.690, 0.577, 0.532. These results suggested that the nitrogen atom of the pyridine ring moiety of **L** was the only reasonable sites for protonation by TNP. To further gain insight into the recognition mechanism, the interaction between the probe **L** and another analogous strong organic acid, such as trifluoroacetic acid (TFA) in solution was also researched by the method of ^{1}H NMR titration (Figure S9, ESI†). The signals of the hydrogens were downfield shifted, especially, Hb and Hc were shifted obviously. These results further confirmed that the ratiometric spectra response of **L** to TNP was attributed to the protonation of the pyridine ring moiety by the acidic behavior of TNP, but not the intermolecular electron or energy transfer. In comparison with TFA, that has acidic character, TNP also has an electron-deficient property, which can protonate the pyridine ring group more easily.

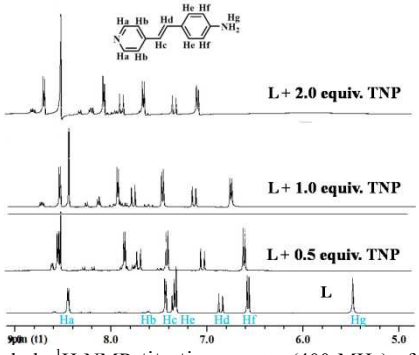

Fig. 4. The whole ^{1}H NMR titration spectra (400 MHz) of the probe **L** with TNP (0, 0.5, 1.0, 2.0 equiv.) in DMSO-d_6.

Theoretical calculation

As shown in Fig. 5, the results revealed that the energy of the highest occupied molecular orbital (HOMO) of the receptor L was -5.03 eV and the energy of the lowest occupied molecular orbital (LUMO) of **L** was -1.15 eV, while the energies of HOMO and LUMO of the newly formed compound **L**·**TNP** were -6.09 eV and -2.99 eV, respectively, which indicated the charge transfer from picrate to the sensor **L**. Meanwhile, the energies of the newly formed compound **L**·**TNP** are minimum, which indicated compound **L**·**TNP** is stable.

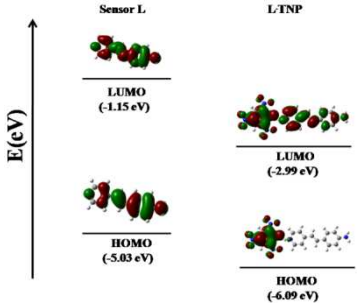

Fig. 5. HOMO and LUMO orbital of receptor L and **L**·**TNP** calculated by B3LYP method with the 6-31G* basis set.

pH effect

In order to understand the selectivity of receptor L toward TNP and/or other NACs, pH effect has been investigated in water. In this case, we selected DNP (pKa = 3.96) as a represent, whose structure is more close to TNP (pKa = 0.71).[28] So the acidity of TNP is stronger than DNP. In other words, TNP would make receptor **L** more easily being protonated. This initial protonation caused an electrostatic association between the picrate anions and the protonated pyridine ends. To confirm this, the effect of pH influence on the UV-Vis response of receptor **L** was examined (Fig. 6a).[29,30] When pH was in the range of 6 to 14, the absorption band centered at 336 nm was unchanged. A decrease of pH from 2 to 1 engendered a blue-shift in the maximum absorption wavelength from 336 nm to 327 nm; this 9 nm shift was due to protonation of the pyridine ring and the amine group to form A-π-A structure. However when pH values changed from 3 to 5, the main absorption peak engendered a red-shift to 396 nm; which was due to protonation of the pyridine ring only, thus enhances the electron-withdrawing effect of the pyridine ring. The effect of pH influence on the fluorescence response of receptor **L** was also examined (Fig. 6b). The receptor **L** was fluorescent on account of the ICT that occurs from the amine group to pyridine ring group. However, when pH range is 1 to 6, the fluorescent intensity reduces significantiy due to the arrest of the ICT process, because of the protonation of either the pyridine ring or the amine group. These results further confirmed that the spectra response of **L** to TNP was attributed to the protonation of pyridine ring group by the acidic behaviour of TNP. And that TNP also had an electron-deficient property which was the main reason that TNP could quench the fluorescence.[31,32]

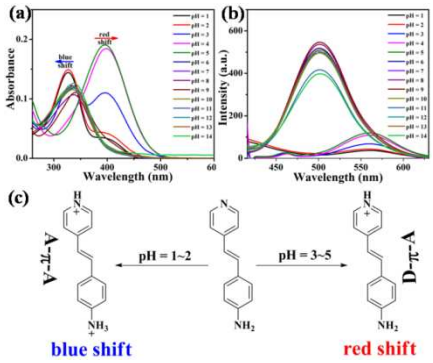

Fig. 6. Effect of pH on the UV-Vis response of **L** in water (a) on the fluorescence response of **L** in water (b) and a scheme of the molecular level interactions involved (c).

Conclusions

In conclusion, we have reported a simple and effective pyridine-based sensor (**L**) for the specific recognition of TNP. The crystal structure of its TNP complex (**L**·**TNP**) was successfully established by X-ray crystallography. In the complex (**L**·**TNP**), picric acid exists as picrate ion upon deprotonation, which leads to quenching of fluorescence of **L.**

Acknowledgments

This work was supported by the National Natural Science Foundation of China (21101001, 50873001 and 61107014), the Educational Commission of Anhui Province of China (no. KJ20142D02).

References

[a] *Department of Chemistry, Key Laboratory of Functional Inorganic Materials of Anhui Province, Anhui University, Hefei 230039, P. R. China.*
[b] *State Key Laboratory Materials, Shandong University, Jinan 502100, P. R. China.*
CCDC: 987872
China.Tel: +86-551-63861279;
E-mail:jxyang@ahu.edu.cn kong-lin2009@126.com

† Electronic Supplementary Information (ESI) available: [details of any supplementary information available should be included here]. See DOI: 10.1039/b000000x/

1. B.W. Xu, X.F. Wu and H.B. Li, Macromolecules, 2011, **44**, 5089.
2. F. Zhang, L. Luo and Y. Sun, Tetrahedron, 2013, **69**, 9886.
3. E.B. Coropceanu, L. Croitor and A.V. Siminel, Polyhedron, 2014, **75**, 73.
4. B.K. Dey, J. Dutta and M.G.B. Drew, J. Organomet. Chem., 2014, **750**, 176.
5. M. Kumar, S.I. Reja and V. Bhalla, Org. Lett., 2012, **14**, 6084.
6. a) V. Bhalla, A. Gupta and M. Kumar, Appl. Mater. Interfaces, 2013, **5**, 672; b) Y. Salinas, R. Martínez-Máñez and M.D. Marcos, Chem. Soc. Rev., 2012, **41**, 1261.
7. a) Y.H. Lee, H.G. Liu and J.Y. Lee, Chem. Eur. J., 2010, **16**, 5895; b) W.S. Zou, F.H. Zou and Q. Shao, J. Photoch. Photobio. A, 2014, **278**, 82.
8. K. Zhang, H.B. Zhou and Q.S. Mei, J. Am. Chem. Soc., 2011, **133**, 8424.
9. G. He, N. Yan and J.Y. Yang, Macromolecules, 2011, **44**, 4759.
10. V. Pimienta, R. Etchenique and T. Buhse, J. Phys. Chem. A, 2001, **105**, 10037.
11. J.Y. Shen, J.F. Zhang and Y. Zuo, J. Hazard. Mater., 2009, **163**, 1199.
12. J.F. Wyman, M.P. Serve and D.W. Hobson, J. Toxicol. Environ. Health. Part A, 1992, **37**, 313.
13. G. Anderson, J.D. Lamar and P.T Charles, Environ. Sci. Technol., 2007, **41**, 2888.
14. X.G. Hou, Y. Wu and H.T. Cao, Chem. Commun., 2014, **50**, 6031.
15. J. Li, J.Z. Liu and B.Z. Tang, RSC Adv., 2013, **3**, 8193.
16. V. Bhalla, S. Kaur and V. Vij, Inorg. Chem., 2013, **52**, 4860.
17. N. Venkatramaiah, S. Kumar and S. Patil, Chem. Commun., 2012, **48**, 5007.
18. G. Sivaraman, B. Vidya and D. Chellappa, RSC Adv., 2014, **4**, 30828.
19. L. Hong, Q.S. Mei and L. Yang, Analytica Chimica Acta, 2013, **802**, 89.
20. M. Jahan, Q.L. Bao and K.P. Loh, J. Am. Chem. Soc., 2012, **134**, 6707.
21. V. Sathish, A. Ramdass and Z.Z. Lu, J. Phys. Chem. B, 2013, **117**, 14358.
22. S. Kumar, P. Singh and A. Mahajan, Org. Lett., 2013, **15**, 3400.
23. V. Bhalla, A. Gupta and M. Kumar, Org. Lett., 2012, **14**, 3112.
24. L.J. Farrugia, J. Appl. Cryst., 1999, **32**, 837.
25. A.L. Spek, PLATON, Acta Cryst. A, 1990, **A46**, C34.
26. Y.Q. Zhang, Y. Guo and Y.H. Joo, Chem. Eur. J., 2010, **16**, 10778.
27. H.L. Liu, X.L. Hou and L. Pu, Angew. Chem. Int. Ed., 2009, **48**, 382.
28. N. Dey, S.K. Samanta and S. Bhattacharya, Appl. Mater. Interfaces, 2013, **5**, 8394.
29. H.P. Zhou, J.Q. Wang and Y.X. Chen, Dyes Pigm, 2013, **98**, 1.
30. S.P. Wu, K.J. Du and Y.M. Sung, Dalton Trans, 2010, **39**, 4363.
31. K.K. Kartha, S.S. Babu, S. Srinivasan and A. Ajayaghosh, J. Am. Chem. Soc., 2012, **134**, 4834.
32. V. Bhalla, S. Pramanik and M. Kumar, Chem. Commun., 2013, **49**, 895.